

# Microchip System for Patterning Cells on Different Substrates via Negative Dielectrophoresis

Kaicheng Huang , Bo Lu , Jiewen Lai , and Henry Kar Hang Chu , Member, IEEE

**Abstract**—Seeding cells on a planar substrate is the first step to construct artificial tissues *in vitro*. Cells should be organized into a pattern similar to native tissues and cultured on a favorable substrate to facilitate desirable tissue ingrowth. In this study, a microchip system is designed and fabricated to form cells into a specific pattern on different substrates. The system consists of a microchip with a dot-electrode array for cell trapping and patterning and two motorized platforms for providing relative motions between the microchip and the substrate. AC voltage is supplied to the selected electrodes by using a programmable micro control unit to control relays connected to the dot-electrodes. Nonuniform electric fields for cell manipulation are formed via negative dielectrophoresis (n-DEP). Experiments were conducted to create different patterns by using yeast cells. The effects of different experimental parameters and material properties on the patterning efficiency were evaluated and analyzed. Mechanisms to remove abundant cells surrounding the constructed patterns were also examined. Results show that the microchip system could successfully create cell patterns on different substrates. The use of calcium chloride ( $\text{CaCl}_2$ ) enhanced the cell adhesiveness on the substrate. The proposed n-DEP patterning technique offers a new method for constructing artificial tissues with high flexibility on cell patterning and selecting substrate to suit application needs.

**Index Terms**—Cell patterning, micro manipulation, negative dielectrophoresis.

## I. INTRODUCTION

TISSUE engineering has gained increasing attention to regenerate damaged tissues and organs by using artificial materials [1]. Cells harvested from patients are seeded on an engineered scaffold, which serves as a 3D substrate for cell proliferation, to construct artificial tissues *in vitro*. The scaffold is then incubated in a bioreactor that regulates the culture environment [2]. Cells on the substrate should be organized or arranged in a pattern similar to the native tissue to facilitate tissue ingrowth. For instance, hepatic lobule, which are the building block of the liver, has a hexagonal shape with hepatocytes arranged in radial lines between interlobular veins. Hence, hepatocytes should be

Manuscript received July 4, 2019; revised August 9, 2019; accepted August 20, 2019. Date of publication August 28, 2019; date of current version November 4, 2019. This work was supported by the Research Grant Council of the Hong Kong Special Administrative Region, China, under Grant 25204016. This paper was recommended by Associate Editor K. C. Cheung. (Corresponding author: Henry Kar Hang Chu.)

The authors are with the Department of Mechanical Engineering, The Hong Kong Polytechnic University, Hong Kong (e-mail: 16903397r@connect.polyu.hk; 15902876r@connect.polyu.hk; jw.lai@connect.polyu.hk; henry.chu@polyu.edu.hk).

Color versions of one or more of the figures in this article are available online at <http://ieeexplore.ieee.org>.

Digital Object Identifier 10.1109/TBCAS.2019.2937744

seeded radially rather than arbitrarily on a hexagon scaffold to construct artificial hepatic lobule.

Forces should be applied to individual cells to manipulate them in a specific form or pattern. Conventional pick-and-place using tweezers would be an inefficient and time-consuming process to handle a large number of cells. Therefore, researchers have examined different non-contact methods for cell handling. The mechanism to manipulate micro-objects can generally be categorized as electrophoresis (DEP) [3], dielectrophoresis [4], optical force [5], magnetic force [6], and hydrodynamic force [7]. Cheng *et al.* [8] employed DEP to pattern molecules and DNAs for force spectroscopy. Messner *et al.* [9] applied a stencil to pattern cancerous cells in an array for analysis. Collin *et al.* [10] used acoustic wave to pattern polystyrene beads onto individual microwells. Yang *et al.* [11] utilized a parallel trapping and optical releasing mechanism to selectively remove trapped particles. Huan *et al.* [12] employed a Honeycomb-like scaffold to fabricate a 3D structure with mammalian cells that mimic the native tissues. Rosa *et al.* [13] combined the DEP and electrodisruption technique to prepare samples for respiratory bacterial pathogens. Among these methods, DEP force manipulation is commonly used in the biomedical field because of its easy setup and simple hardware requirements for experiment. Moreover, DEP force manipulation can be applied to any type of biological cells, which are polarizable in nature, without the need of pretreatment, thereby eliminating potential hazards to the cells.

DEP involves dielectric particles in a non-uniform electric field, where they experience translational force due to the polarization effect [14]. This phenomenon was first recognized and explored by Pohl [15]. The direction of the force acting on the particle is dependent on the gradient of the electric field, the frequency of the applied electric field, and the dielectric properties of the particle and medium. The movement of particles from the weak toward the strong electric field region is referred to as positive DEP (p-DEP), whereas the reverse process is negative DEP (n-DEP). A number of electrode configurations, such as castellated [16], curved [17], quadrupole [18], microwell [19], spiral [20], extruded [21], interdigitated [22], sidewall [23], and insulator-based or electrodeless designs [24], applications in cell trapping [25]–[27], positioning [27], separation [28], and patterning [26], [27], [29]–[31], have been examined to generate nonuniform electric fields.

Studies have focused on using n-DEP to reduce the invasiveness for cell manipulation and minimize the effect of high electric fields on cell viability. Kim *et al.* [32] used an electrode

pair to trap cells within a microfluidic environment. The trapped cells were then cultured to observe their viability, but the cells have to be incubated within the channel. Suzuki *et al.* [29] used a sandwiched microchannel design consisting of upper parallel electrodes and a bottom ground substrate to pattern colloidal particles onto the low electric field regions of the substrate by n-DEP force. Using the same technique, they enhanced the chip design to create alternating cell lines from two cell types on a substrate [30]. In these studies, cross-linkers or photosensitive hydrogels were used to immobilize the patterned cells before substrate detachment. Also, the cell pattern to be constructed is dependent on the electrode design and cannot be changed after the device fabrication. Ino *et al.* [26] considered a multi-layer electrode design to create dot patterns on the surface of the microchannel via n-DEP. They concluded that the height of the microchannel would inversely affect the quality of the dot patterns. Yafouz *et al.* [31] applied microarray dot electrodes to create cell patterns, and each electrode can be energized through individual input pins. Couniot *et al.* [33] utilized CMOS technology to fabricate a biosensor array, and this chip can be used to detect a single bacterial cell. Nevertheless, the majority of the research mainly focuses on utilizing an electrode array for high throughput cell patterning or precise cell manipulation, but not for constructing different cell patterns for the intended applications.

Selection of the substrate material for cell seeding is important to provide a suitable culture environment for cells. Polymeric materials are commonly used because they are biocompatible and can be easily processed into different sizes and shapes. Natural polymers (e.g., collagen, decellularized arterial matrix, fibrin, alginate, hyaluronate, and chitosan) and synthetic polymers (e.g., polystyrene, poly-l-lactic, polyglycolic acid [34], poly-dl-lactic-co-glycolic acid and PEDGA [35]) are biomaterials used for scaffold fabrication.

Hydrogel substrates are promising alternatives because of their high tissue-like water content, high permeability, and tunable properties. In addition, cells can be added to the aqueous hydrogel solution for direct cell encapsulation and patterning. The aqueous solution should be physically or chemically crosslinked to cure hydrogel into solid form. Physical crosslinking involves the use of radiant energy, temperature, enzyme, or other noncovalent methods to enable physical interactions between polymer chains. Chemical crosslinking involves the use of chemical agents and solvents to synthesize permanent, chemical links among molecular chains. Patterning and gelation are often conducted sequentially through a microfluidic chip to immobilize the cell pattern for subsequent culture. Warm aqueous agarose solution with cells are first supplied to a microfluidic chip for DEP patterning, and gelation is activated by cooling the solution to room temperature [36]. Aqueous PEDGA solution can be mixed with cells and photoinitiator to trigger the crosslinking of polymer chains in a short period of time under UV irradiation [37]. However, several issues should be considered when selecting hydrogel as the substrate material. Cell viability would be a concern if the hydrogel-containing cells are crosslinked at extreme temperature or condition. Chemical agents for crosslinking, whether hazardous or not to the cells,

would also be a concern during culture. Therefore, separating the patterning and gelation procedure, patterning cells on a existing hydrogel would be a better choice for increasing the cell viability.

In our previous work, we first proposed a microchip design for patterning cells onto a glass substrate [39]. This microchip consisted of a dot-electrode array design and was fabricated using printed circuit board technology. In [38], multiple relays were connected to the microchip to energize individual dot-electrodes to generate different electric fields for cell patterning. The microchip was also mounted on a height adjustable platform for precise control of the distance between the microchip and the substrate. In this study, we aim to further enhance the functionality of the microchip system for patterning different cell patterns on various substrates. The mechanism for cells to adhere to the substrate was first examined to optimize cell attachment. Yeast cells were selected for the experiments because of their dielectrophoretic behavior similar to mammalian cells [40]. Since most of the substrates are transparent, Janus Green B was used to stain the cells to enhance the contrast for better illustration. Two different configurations were proposed for efficient cell patterning. The microchip on the microscope system was configured as a microchannel or a movable platform. A series of experiments was conducted to compare the patterning performance between the two configurations and determine their effectiveness for patterning on various substrates.

The paper is organized as follows. Section II provides the theory related to cell patterning and cell adhesion. Section III describes the materials and experimental methods. Section IV presents the results and discussion. A summary is given at the end of this article.

## II. THEORY

### A. Cell Manipulation via DEP

The principle of DEP is the use of nonuniform electric fields to induce polarization in an electroneutral particle to manipulate the particle to the high or low electric field region. According to Pohl [15], the DEP force,  $F_{DEP}$ , acting on a spherical body is given by:

$$F_{DEP} = 2\pi r^3 \varepsilon_m \cdot Re[K(\omega)] \cdot \nabla E^2 \quad (1)$$

where  $r$  is the particle radius,  $\varepsilon_m$  is the permittivity of the suspending medium,  $\nabla$  is the Del vector operator, and  $E$  is the root mean square of electric field. The Clausius–Mossotti (CM) factor represents the interaction between the particle and the medium, and its real part,  $Re[K(\omega)]$ , can be evaluated as:

$$K(\omega) = \frac{\varepsilon_p^* - \varepsilon_m^*}{\varepsilon_p^* + 2\varepsilon_m^*} \quad (2)$$

where  $\varepsilon_p^*$  is the complex permittivity of the particle and  $\varepsilon_m^*$  is the complex permittivity of the suspension medium.

For biological specimens, Huang *et al.* [41] proposed a smeared-out approach to represent a multi-shell particle as a homogeneous particle. The inner (layer 1) and the adjacent layer (layer 2) are remodeled as a homogeneous particle, and the equivalent electrical properties can be evaluated and progressed layer-by-layer toward the outermost layer (layer N). The

TABLE I  
PROPERTIES OF YEAST CELL [41] AND 1M AHA MEDIUM [42]

	Viable yeast cell			Non-Viable yeast cell			Medium
	Cytoplasm	Cell membrane	Cell wall	Cytoplasm	Cell membrane	Cell wall	
Conductivity $\sigma(\mu\text{S}/\text{cm})$	$2 \times 10^3$	$2.5 \times 10^{-3}$	$1.4 \times 10^2$	70	1.6	15	40
Relative permittivity $\varepsilon$	$60\varepsilon_0$	$6\varepsilon_0$	$50\varepsilon_0$	$60\varepsilon_0$	$6\varepsilon_0$	$50\varepsilon_0$	$160\varepsilon_0$
Radius $r(\mu\text{m})$	2.5	$8 \times 10^{-3}$	$2 \times 10^{-2}$	2.5	$8 \times 10^{-3}$	$2 \times 10^{-2}$	

equivalent complex permittivity of the first two layers can be represented as:

$$\begin{aligned} \varepsilon_{1,e}^* = S(\varepsilon_1^*, \varepsilon_2^*, R_1, R_2) &= \varepsilon_2^* \left[ \left( \frac{R_2}{R_1} \right)^3 + 2(\varepsilon_1^* - \varepsilon_2^*) \right. \\ &\quad \left. / (\varepsilon_1^* + 2\varepsilon_2^*) / \left[ \left( \frac{R_2}{R_1} \right)^3 + 2(\varepsilon_1^* - \varepsilon_2^*) / (\varepsilon_1^* + 2\varepsilon_2^*) \right] \right] \end{aligned} \quad (3)$$

where  $\varepsilon^*$  and  $R$  are the complex permittivity and the radius of the first two layers, respectively.

Common baker's yeast can be modeled as a two-shell (three layers) particle as follows:

$$\varepsilon_p^* = S(S(\varepsilon_{cyto}^*, \varepsilon_{mem}^*, R_{cyto}, R_{mem}), \varepsilon_{wall}^*, R_{mem}, R_{wall}) \quad (4)$$

Equation (4) shows that, the sign of the CM factor signifies the direction of the DEP force, which is dependent on the electrical properties of the cell and the medium, as listed in Table I. However, these two properties are related to the application and cannot be changed. The operating frequency of the input signal,  $\omega$ , can be adjusted to determine the sign of the CM factor. n-DEP force is required to pull the cells to arrange and pattern them onto the substrate. Based on the simulation, the crossover frequency was evaluated to be 4.2 MHz and the signal frequency was set to 6 MHz to induce n-DEP force for dead yeast cell manipulation. For manipulation of live yeast cells, two crossover frequencies were simulated to be 47 kHz and 42 MHz respectively, and a low frequency of 30 kHz was chosen for n-DEP cell manipulation.

### B. Cell Adhesion to the Substrate

The interaction between the cells and the substrate should be established for cells to adhere to the surface. The inside of a biological cell is negatively charged compared with the outside of the plasma membrane because of the ion diffusion between the intracellular and extracellular fluids under resting conditions. Cell attachment via electrostatic interaction can be promoted by altering the surface of the substrate by using reagents, such as polymers of D- and L-lysine. These reagents can increase the number of positively charged surface ions for binding. With the coating, yeast cells on the glass surface effectively resisted being washed under tap water [43]. On the cell surface, many receptors, including integrins and adhesion molecules, can mediate adhesion to the substrate and nearby cells. For *Saccharomyces cerevisiae* (yeast) considered in this study, the protein receptor that is responsible for cell adhesion is adhesins, which consists of three domains: C-terminal, middle domain, and N-terminal.

The C-terminal domain serves as the root that connects the adhesion to the cell surface. The middle domain contains short amino acid repeats as the main body. The N-terminal domain specifies the two main types of binding, namely, lectin-like and sugar-insensitive adhesion. Lectin-like adhesins contain a carbohydrate binding domain that facilitates binding to sugar residues on the cell surface. Sugar-insensitive adhesins have n-terminal that can bind to peptides to increase the surface hydrophobicity, promoting hydrophobicity-based adhesion between the cells and abiotic surfaces [44]. Calcium ion can be added to promote cell-cell adhesion (flocculation) and attachment to substrates in an acidic environment [45], [46].

Another factor that influences cell attachment is the material surface. A larger surface area for contact allows more bonds to form between the cell and the surface, leading to strengthened adhesion. The interaction between the surface roughness and the cell can be explained by attachment point theory [47]. When the roughness scale is smaller than the cell, the attachment can be considered a multi-point attachment, which provides strong adhesion. As the roughness scale increases, the number of attachment points decreases, resulting in reduced adhesion force. When the cell size is comparable with the roughness, the cell falls into the valley and the contract changes back to the multi-point attachment. To date, several groups have examined the effect of surface roughness on cell adhesion, but no consensus has been reached. Singh *et al.* [48] cultured osteoblasts on nanostructured cubic zirconia and concluded that increasing the roughness from 19.9 nm to 29.7 nm reduced the cell attachment. Anselme [49] also found that preosteoblast cells were cultured better on a smoother surface. Deligianni *et al.* [50] studied the adhesion of human bone marrow cells to the hydroxyapatite substrates; they showed that the number of adherent cells per unit surface increased with increasing surface roughness. Giljean *et al.* [51] cultured human osteoblasts in titanium alloy with different roughness values. Surface roughness between 0.01 and 0.1  $\mu\text{m}$  did not significantly influence the cell adhesion mechanism. Huang *et al.* [52] reported that osteoblast-like U2-OS cells adhered better on the Ti surface with 0.15  $\mu\text{m}$  roughness than on rougher (1.2  $\mu\text{m}$ ) or smoother (0.05  $\mu\text{m}$ ) surfaces. In addition to surface roughness, the optical density, which is affected by the powders used for surface polishing, should be considered.

## III. MATERIALS AND METHODS

### A. Preparation of Cells and Culture Media

Yeast cell was selected for examining cell patterning via n-DEP. Active dry yeasts (Pan Pacific Active Dried Yeast) were activated in Deionized (DI) water with sucrose (9% w/w). The

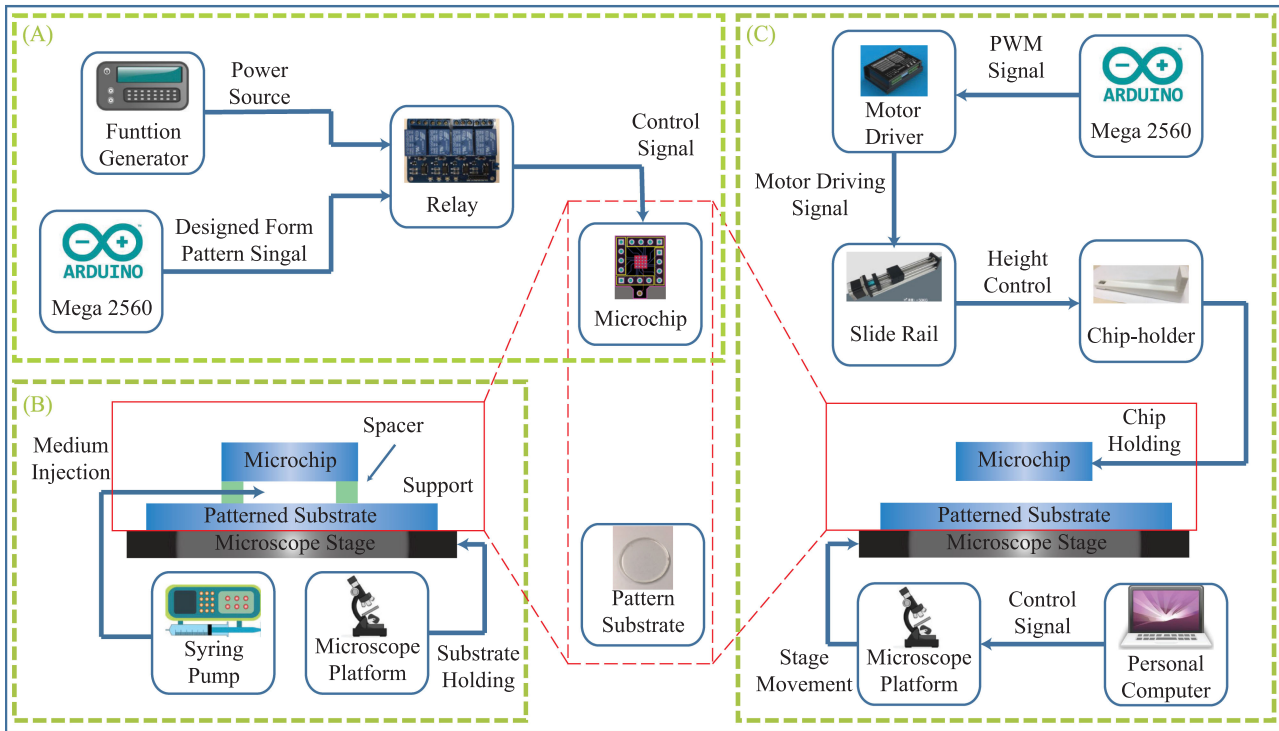


Fig. 1. Schematic of the microchip system: (A) controllable microchip; (B) microchannel configuration; and (C) movable platform configuration.

cell solution was incubated at 35 °C for 1 h. The dead yeast cells were prepared by heating half of the cell solution at 90 °C for another 30 min. The cell solutions were rinsed four times with PBS and diluted to prepare multiple samples of live and dead yeast cells. Janus green B (Shanghai MAIKUN Chemical Co., Ltd) was used to enhance the contrast between the cells and the background for viewing under microscope. The dead cells were stained for 30 min to allow more uptake of the dye. After staining, the samples were washed again four times with PBS, and the live and dead cells were resuspended in DI water, 6-aminohexanoic acid (AHA) (Ruibio) solutions, and calcium chloride solutions (International Laboratory, USA) for the experiments.

### B. Preparation of Substrates

Various materials, namely, glass, PDMS, PMMA and PVC were prepared as substrates. These materials were chosen because of their biocompatibility. Moreover, these materials are commonly used to fabricate Petri dishes and labware for cell culture. Standard glass slides were used as the glass substrate. PMMA sheets with 0.2 mm thickness were purchased and cut into multiple substrates (20 mm × 20 mm). PVC Petri dishes were purchased (Corning, USA). PDMS sheets were prepared using Sylgard 184 Silicone Elastomer Kit. The elastomer-to-curing agent ratio was 10:1, and the curing process was conducted in an oven at 60 °C for 1 h. Prior to the experiment, all substrates were cleaned in an ultrasonic cleaner for 5 min.

### C. Experimental Setup for Cell Patterning

The core component of the system is a microchip that can manipulate cells into various patterns. Details on the design

and fabrication of the microchip are described in [39]. In brief, this microchip utilizes a 3.5 mm × 3.5 mm PCB plate as the surrounding electrode with 16 holes of diameter 700 μm arranged in a “4 × 4” manner. Sixteen circle electrodes with a diameter of 400 μm are concentrically aligned with the holes on the plate, forming electrode pairs for cell manipulation via dielectrophoresis.

The microchip system used for cell patterning, which can be configured as a microchannel or movable platform, is illustrated in Figs. 1 and 2. Particular cell pattern can be constructed on the substrate by using multiple relays to control the voltage supply between the individual electrodes of the microchip and the function generator (Fig. 1A). An Arduino micro controller board was used to program the relays to turn on or off the voltage supply to each pin based on the cell pattern. Depending on the application, the microchip of the system can be secured firmly in a microchannel configuration or displaced through a movable platform.

For the microchannel configuration, the system consists of four main components, namely, a Leica inverted microscope, a dual syringe pump, a microchip, and a slice of the material substrate (Fig. 1B). Two 100 μm spacers were sandwiched between the microchip and the substrate to form a channel for the cell solution to flow through. The inlet and outlet of the channel were connected to a dual syringe pump, where the cell-containing medium was injected from one syringe and collected by the other syringe.

The patterning protocol can be summarized in five steps. First, the yeast cells were resuspended in AHA solution and injected into the gap between the microchip and the substrate (Fig. 3A).

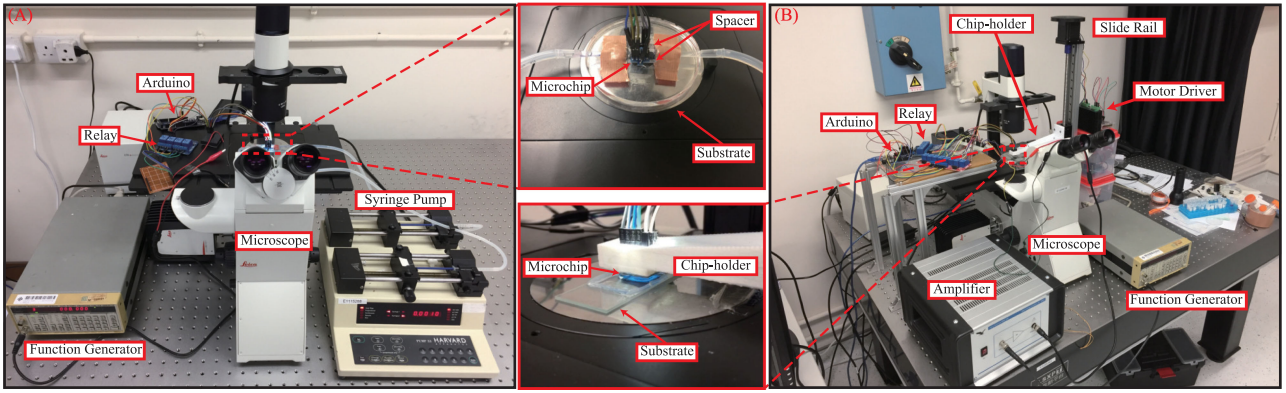


Fig. 2. Experimental setup of the microchip system in (A) microchannel and (B) movable platform configurations.

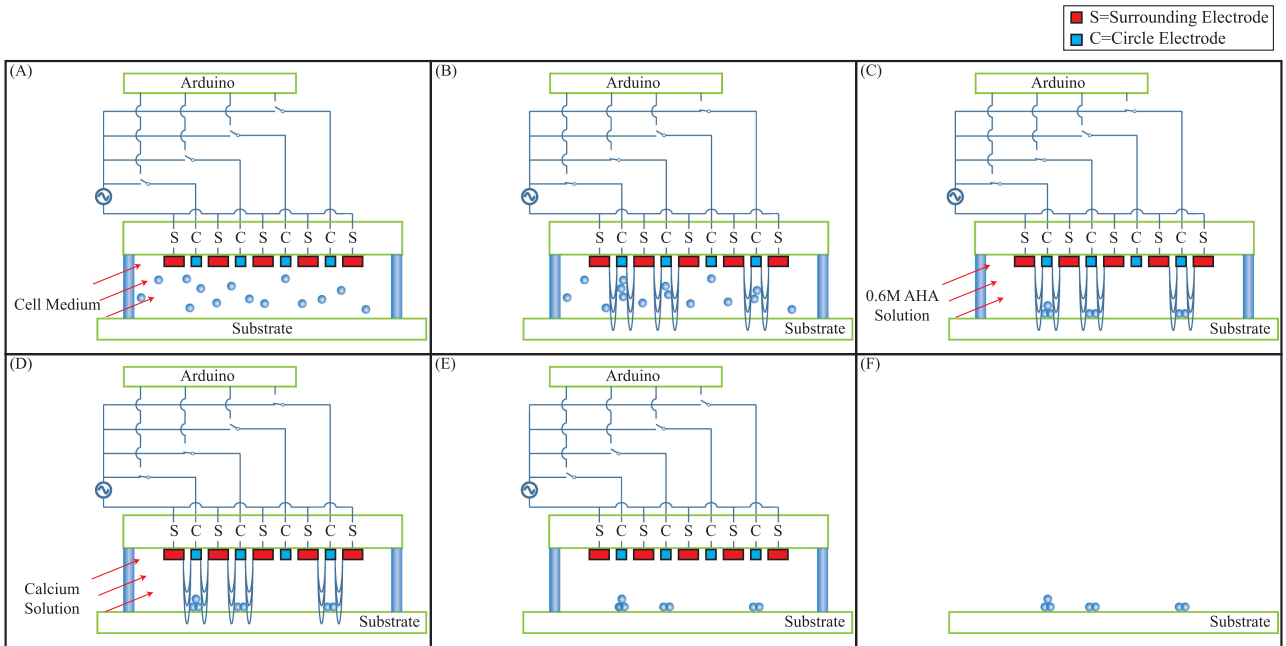


Fig. 3. Cell patterning procedure with microchannel configuration: (A) Cell solution was injected into the channel; (B) Individual electrode pairs were energized to concentrate the cells; (C) 0.6M AHA solution was injected for pattern transfer; (D) Calcium solution was injected to enhance cell adhesion; (E) The electrodes were de-energized; (F) The microchip and the spacers were removed, leaving the substrate with cell pattern.

The dot electrodes were energized based on the specified cell pattern to create the electric field (Fig. 3B). Afterward, the cell-free medium with lower molarity AHA was injected into the channel to wash away the cells unaffected by n-DEP. Meanwhile, the change in the relative density between the cell and medium resulted in the transfer (sedimentation) of the cell pattern onto the substrate surface (Fig. 3C). This step effectively reduced the number of cells on the final pattern.  $\text{CaCl}_2$  solution was injected into the channel after the abundant cells were washed to strengthen the adhesion between the cells and substrate (Fig. 3D). Finally, the electric fields were de-energized until the patterned cells firmly adhered to the substrate (Fig. 3E). The microchip was then removed (Fig. 3F).

For the movable platform configuration, the microenvironment between the substrate and the microchip can be freely

adjusted by two motorized platforms [38] rather than fixed by two spacers. The microchip is attached to the slide rail through a 3D printed chip-holder, while the substrate is secured on a motorized stage to be manipulated with respect to the microchip for large-scale cell patterning. A control interface was developed using C++ program, which can display images from the microscope to facilitate coordinated movements among the slide rail, the motorized stage, and the objective lens. The complete system setup is shown in Fig. 1C.

Similar to the microchannel configuration, yeast cells in the AHA solution were used and a large droplet was dispensed on the substrate. The microchip on the rail was lowered to completely immerse in the cell solution at  $100 \mu\text{m}$  above the substrate (Fig. 4A). The fluid flow in between the microchip and substrate was limited due to surface tension. Then, a large amount of

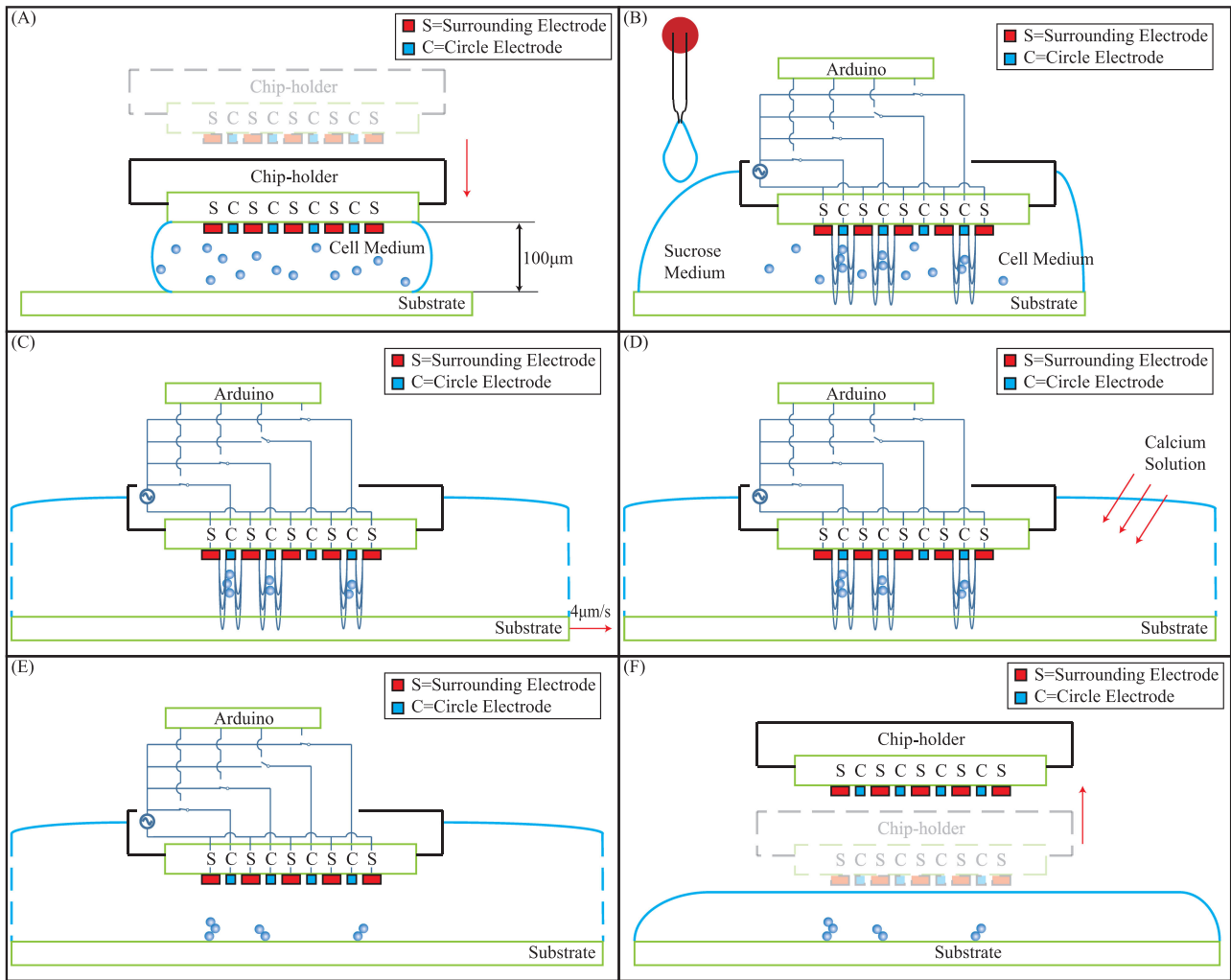


Fig. 4. Cell patterning procedure with movable platform configuration: (A) Cell solution was dropped on the substrate, and the microchip was moved down with 100  $\mu\text{m}$  gap to the substrate; (B) Sucrose medium was dispensed adjacent to the cell solution. Individual electrode pairs were energized for concentrating cells; (C) The substrate was moved by the platform such that the patterned cells were transferred to the clean area; (D)  $\text{CaCl}_2$  solution was injected to enhance cell adhesion; (E) The electrodes were de-energized; (F) The microchip was moved up, and the substrate with redundant cells was removed, leaving the substrate with the cell pattern.

droplet of sucrose in deionized (DI) water (9% w/w) was dispensed adjacent to the cell solution to provide a cell-free region. Depending on the pattern, the electrodes on the microchip were selectively powered on to create the cell pattern (Fig. 4B). The platform was then moved at 4  $\mu\text{m}/\text{s}$  to transfer the cell pattern trapped by the microchip from the cell-containing region to a clean region of the substrate for patterning (Fig. 4C). Afterwards, the  $\text{CaCl}_2$  were slowly added into the solution to enhance the cell adhesion on the substrate (Fig. 4D). Finally, the electric fields were de-energized until the patterned cells firmly adhered to the substrate (Fig. 4E). The microchip was then moved upward (Fig. 4F). Changing the substrate and the energized electrodes leads to different characters on different substrates.

#### IV. RESULTS AND DISCUSSION

The performance of the microchip for patterning cells on different substrate materials was evaluated through experiments.

As discussed in Section II, the quality of the cell pattern is highly correlated with n-DEP and adhesion forces. The strength of these forces is affected by several parameters, namely, medium of the cell solution, material properties of the substrate, and signal inputs to the microchip. Different tests were conducted to examine the effects of individual parameters and optimize them. Unless otherwise specified, all tests were performed using dead yeast cells in AHA solution with a cell concentration of  $1.2 \times 10^8$  cells/mL.

##### A. Effect of the Medium on Cell Attachment

*1) Density:* The density of the cell medium is one of the factors influencing the quality of the cell pattern. Cells gradually sink to the bottom because of gravitational force. Once the cells become in contact to the substrate surface, the cells start to flatten on the surface and the adhesion force prevents the cells from further motion. If the cells are suspended in a medium

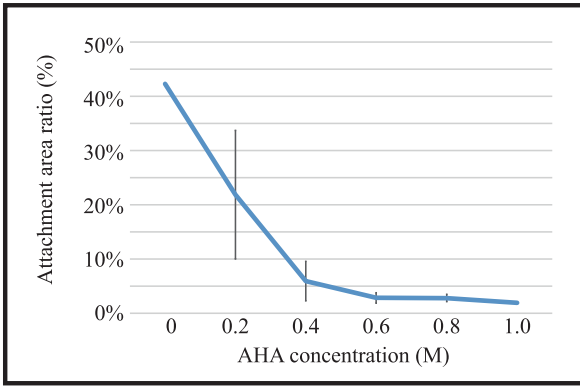


Fig. 5. Effect of AHA concentration on yeast cell adhesion.

denser than the cells, then high buoyancy force could help levitate the cells, resulting in a longer time for the formation of the cell pattern. In this work, the yeast cells have a density of approximately  $1.1126 \text{ g/cm}^3$ . Different amounts of AHA powders were dissolved in DI water to prepare solutions with molarities from 0 M to 1 M (molecular weight: 131 g/mol) to suspend the yeast cells for evaluating the effect of the medium density. The cell attachment test was conducted using a glass substrate to construct a microchannel with a height of  $100 \mu\text{m}$ . The yeast cells in different AHA solutions were injected into the channel. The solution in the channel was left idle. After 8 minutes, the channel was washed with cell-free AHA solution. Images of the substrate before and after washing were captured and used to compute the cell attachment rate. ImageJ was used to count the area occupied by the cells (Fig. 5). Increasing the molarity (M) of the AHA solution can effectively prevent the cells from attaching to the substrate surface. As the molarity increases, the density of the solution also increases, providing larger buoyancy force to reduce the speed of cell sediments. Adjusting the medium density can enable cells to remain in suspension for cell patterning via DEP.

2) *Calcium Chloride*: As discussed in Section II, calcium ions enhance the ability of cell adhesion. Solutions with different  $\text{CaCl}_2$  concentrations were used in the experiments to examine the effectiveness of calcium ions in the patterning process. From the previous results, pure DI water led to over 40% of cell attachment, and the enhancement with calcium ions may not be obvious. Hence, 0.5 M AHA solution ( $1.0135 \text{ g/cm}^3$ ) was chosen as the base solution, and  $\text{CaCl}_2$  was added to prepare solutions with molarities ranging from 0.5 mM to 2.5 mM.

$\text{CaCl}_2$  significantly affected cell adhesion (Fig. 6). As more  $\text{CaCl}_2$  was added to the solution, more cells were attached and remained adhered onto the substrate. When the molarity increased to 2.5 mM, the substrate was almost completely covered by cells. This result confirms the findings in [46] that calcium ions could enhance the adhesion of yeast cells to the substrate. Therefore,  $\text{CaCl}_2$  in the solution was used in the last step of all experiments for stabilization of yeast cells.

#### B. Effect of Substrate on Cell Attachment

1) *Hydrophobicity*: Hydrophobicity is the tendency of a substrate to repel water molecules and is dependent on the surface

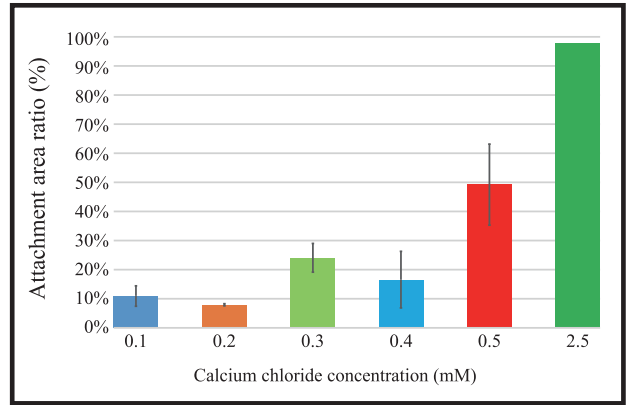


Fig. 6. Effect of calcium chloride concentration on yeast cell adhesion.

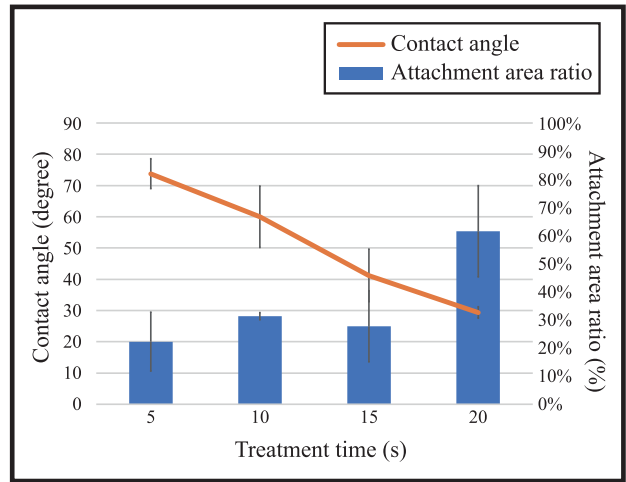


Fig. 7. Contact angle of PDMS substrates after plasma treatment and the effect of substrate hydrophobicity on yeast cell adhesion.

chemistry and the roughness of the material. This property has a strong influence on the cell attachment rate. A hydrophilic surface will lead to higher surface free energy, promoting the cell attachment. Four PDMS substrates with the same material properties were fabricated and used to examine the relationship between hydrophobicity and cell attachability. The substrates were modified by treating in an Expanded Plasma Cleaner (Harrick Plasma, USA) for 5, 10, 15, and 20 s to induce polar functional groups on the surface and change the property from hydrophobic to hydrophilic. Afterward, the substrates were examined with the cell attachment test, and contact angles were measured using a water droplet and microscope.

Plasma treatment effectively modified the substrate surface (Fig. 7). When the substrate was exposed to the cleaner for a longer duration, the measured contact angle decreased, indicating a hydrophilic surface. The cell attachment test showed that hydrophilic PDMS substrates with lower contact angle tended to attach more cells to the substrate. This relationship between material hydrophobicity and cell attachment agrees with a previous report [53]. In order to maintain the hydrophobicity for a longer time, the substrate surface can be treated

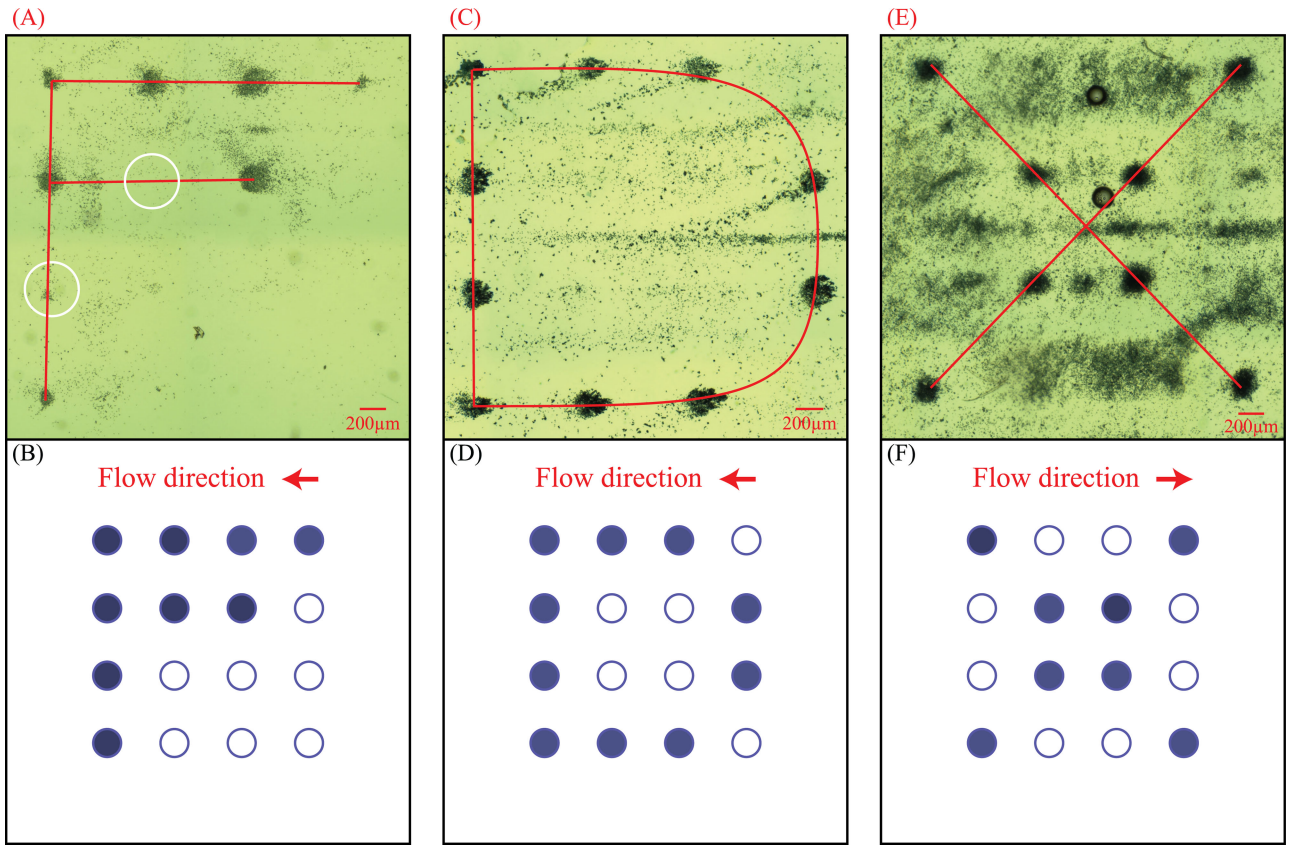


Fig. 8. Patterns observed from the microscope with microchannel system and the corresponding inputs on various substrates (A, D) glass; (B, E) PMMA; (C, F) PDMS.

for longer than 300 s or stored in water before use. [54] Cell attachment is not only dependent on material hydrophobicity but also on surface roughness and cell type. Dong *et al.* [55] examined the attachment of human liver hepatocellular carcinoma cells (HepG2) and mouse osteoblastic UMR106 cells on zein electrospun nanofibrous network. The hydrophobicity effect on cell attachment was observed in one cell type but not on the other cell type. Mercier-Bonin *et al.* [56] revealed the shape and mass of the cell altered the surface hydrophobicity of yeast cells, affecting their attachment rate to the substrate. Dowling *et al.* [57] also reported that the optimal contact angle for attaching MG63 cells is 64°, and a rougher surface can enhance the cell attachment. Nevertheless, the result also shows that surface modification through grinding with SiC paper would not only increase the roughness, but the wettability (contact angle) would also increase as well. These results indicate that cell attachment rate may not be solely dependent on hydrophobicity.

2) *Material Properties:* Different substrates could possess large variations in terms of surface chemistry and roughness because of the nature of the materials and fabrication techniques, leading to a combination effect on the cell attachment. According to previous experimental results, modifying the surface hydrophobicity may not be an effective method to enhance cell adhesion to various substrates. Therefore, the use of CaCl<sub>2</sub> to enhance the cell adhesion on three different

TABLE II  
RELATIONSHIP BETWEEN YEAST CELL ADHESION AND DIFFERENT MATERIAL SUBSTRATES IN AHA SOLUTION AND AHA + CaCl<sub>2</sub> SOLUTION

Material	Glass	PDMS	PMMA
Contact angle	17.8°	79.9°	63.0°
Attachment area ration (0.5 M AHA)	25.14%	14.47%	10.09%
Attachment area ration (0.5 M AHA + 2.5mM CaCl <sub>2</sub> )	97.55%	85.54%	91.60%

substrates, namely, glass, PDMS, and PMMA, were examined. The material properties were measured before the cell attachment experiment (Table II). The glass substrate is hydrophilic, but the other substrates are hydrophobic. The cell attachment test showed that the attachment rate was approximately 10%–25%. When CaCl<sub>2</sub> was added to the medium, the attachment ratio significantly increased to at least 85% in the three substrates, showing that a strong interaction was established between the cell and the substrate. This phenomenon indicates that using CaCl<sub>2</sub> is an effective method to promote the patterning and attachment of yeast cells to different kinds of substrates.

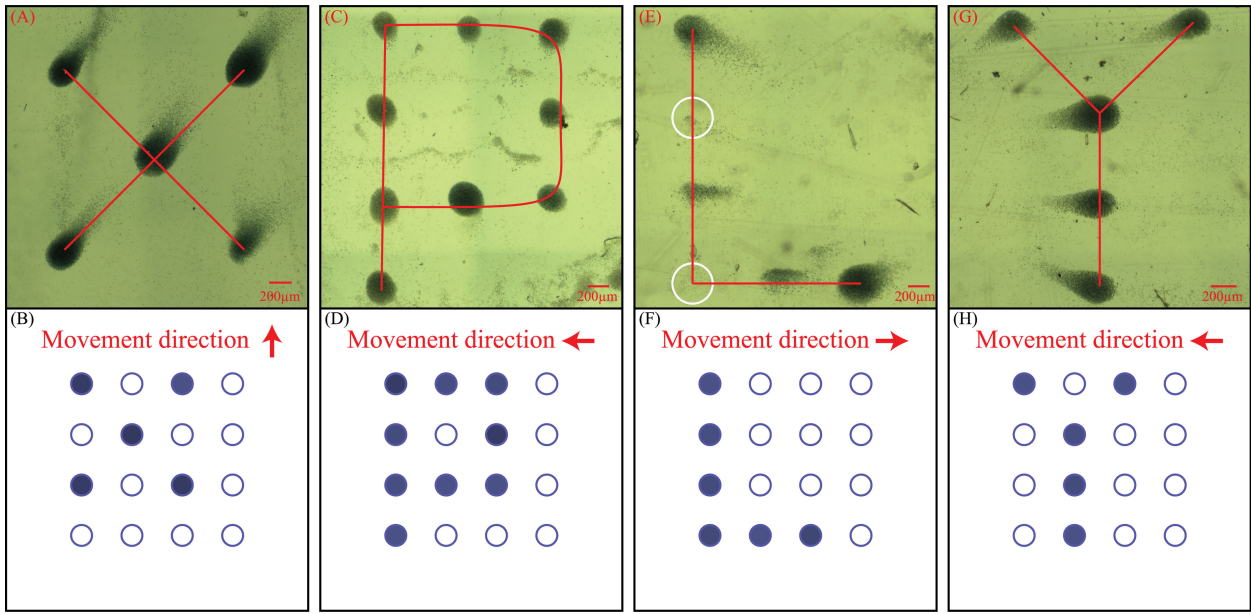


Fig. 9. Patterns observed from the microscope with movable platform configuration and the corresponding inputs on various substrates: (A, B) glass; (C, D) PMMA; (E, F) PDMS; and (G, H) PVC.

### C. Cell Patterning With Different Configurations

1) *Microchannel Configuration:* Various dot patterns were considered to be printed on the substrates by using the 4-by-4 electrode array to examine the effectiveness of the microchip system for cell patterning (Figs. 8B, D, and F). The cell solution was injected through a syringe pump at a flow rate of  $20 \mu\text{L}/\text{min}$ , and a  $60 V_{pp}$  AC voltage at 6 MHz was supplied via the function generator to the microchip. Following the six-step patterning procedure as described, the dot patterns were printed on the glass, PMMA, and PDMS substrates; the corresponding images from the microscope are shown in Figs. 8A, C, and E. The microchip effectively created different cell patterns, and the yeast cells were successfully printed on all the three substrates. It was also noticed that some unpattered yeast cells were scattered around the patterns. The cell dot size on the glass substrate was the smallest among the substrates. As the dot size became denser, the abundant cells on the surrounding increased. This phenomenon suggests the influence of substrate properties on the quality of the overall cell pattern. For the glass substrate, the abundant cells could be easily washed away (Fig. 8A) by flushing cell-free medium in the microchannel. Nevertheless, parts of the constructed cell pattern could also be removed (as shown in white circles) simultaneously. In addition, material hardness affected the efficiency of cell washing. More cells adhered to the soft PDMS substrate than to the hard PMMA substrate. One factor for this phenomenon is the leakage in the microchannel. The spacers used in the study could provide good adhesion between the microchip and harder substrates but not on softer substrates, leading to inefficient fluid flow to wash away abundant cells.

2) *Movable Platform Configuration:* Motorized platforms were incorporated to provide relative motions between the microchip and the substrate to resolve the challenge in removing

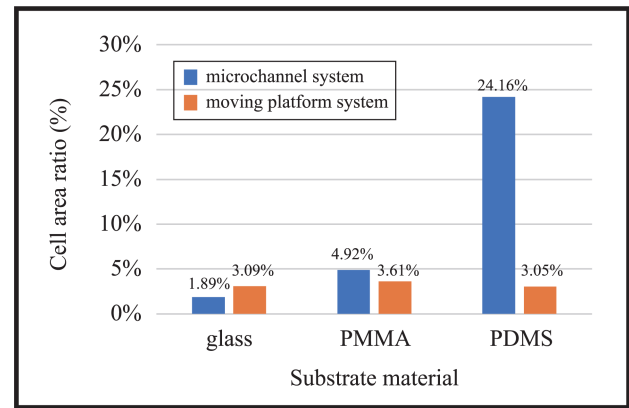


Fig. 10. Cell patterning performance versus different materials with different methods.

abundant cells and extending the flexibility of the microchip for cell patterning. After forming the cell pattern by the microchip, the pattern was dragged from the cell-containing region to the cell-free region on the substrate. Thus, the washing step can be neglected. Compared with washing, the proposed method can significantly reduce the number of abundant cells around the cell pattern.

The performance of cell patterning through the movable platform on glass, PMMA, PDMS, and PVC substrates are shown in Figs. 9A, C, E, and G, respectively. The constructed cell patterns (different characters) were printed more clearly on the different substrates compared with the results in Fig. 8. Approximately no abundant cells were found on the glass, PMMA, and soft PDMS substrates. The ratio of the non-patterned area covered by the cells (i.e., area outside the circles with a  $200 \mu\text{m}$  radius around the cell dots) was measured to evaluate the effectiveness

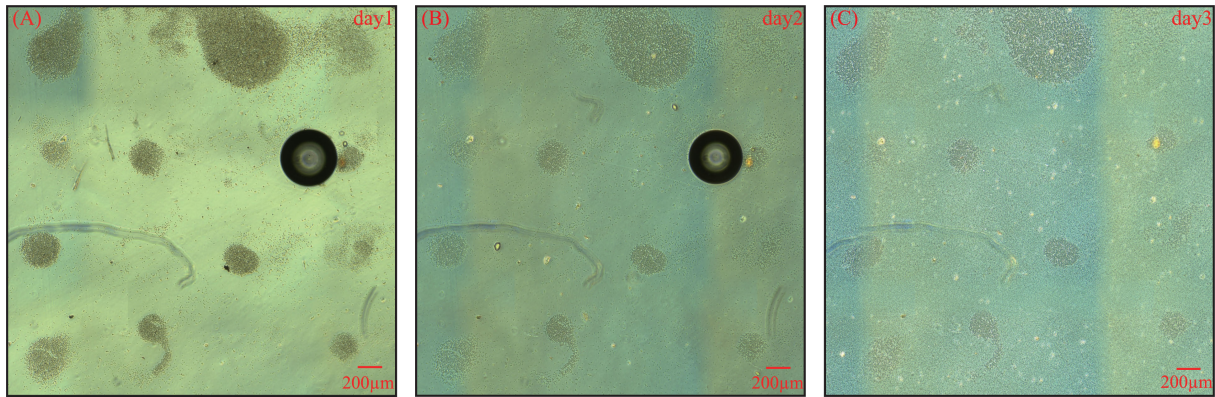


Fig. 11. Yeast cells culturing performance after patterning: (A) day 1; (B) day 2; and (C) day 3.

of the proposed method (Fig. 10). The movable platform could maintain approximately 3% of cell area ratio, irrespective of the substrate material. The quality of the cell dot was influenced by two factors. First, even through a linear rail, the removal of the microchip immersed in the medium could still induce undesired fluid flow on the surface of the substrate. Second, given that the trapped cells were displaced to a new position for patterning, slight angular misalignment between the microchip and the substrate could change the channel height between the cell-containing region to the cell-free region. This phenomenon reduced the strength of the electric fields for cell patterning (white circle shown in Fig. 9E).

#### D. Assay of Cell Viability

Live yeast cells were first patterned on a PVC Petri dish through the movable platform system and incubated at 37 °C to examine cell viability. The medium for patterning was changed to DEP buffer medium (8.5% w/w sucrose, 0.3% w/w glucose) to maintain high viability and patterning efficiency. After patterning, the yeast cell culture medium, that is, Sabouraud Dextrose Broth containing 0.6 mM CaCl<sub>2</sub>, was added in the fourth step. The images of the constructed pattern after 3 days of culture are shown in Fig. 11. The cell pattern retained its shape after 1 day of culture, and the surrounding areas were gradually filled with proliferated yeast cells. After 3 days, newly grown non-adherent yeast cells were detached from the original cells to cover the empty space on the Petri dish (Fig. 11C).

#### V. CONCLUSION

In this study, a microchip was developed for constructing different cell patterns as needed via n-DEP. The microchip was mounted on a motorized platform to enable relative movement with respect to the substrate for efficient cell patterning. Experiments were conducted to evaluate the influence of different experimental parameters on the patterning process. Different cell patterns were successfully printed on different material substrates. Mechanisms to remove abundant cells surrounding the patterns were examined. Addition of CaCl<sub>2</sub> in the medium enhanced the adhesion force and led to firm attachment of the yeast cells to the substrates after detachment. Cell culture

was conducted to confirm cell viability after patterning. The proposed microchip system offers a simple yet effective solution to create different cell patterns on a number of substrates for tissue engineering applications.

#### REFERENCES

- [1] C. A. Vacanti, "History of tissue engineering and a glimpse into its future," *Tissue Eng.*, vol. 12, no. 5, pp. 1137–1142, 2006.
- [2] K. Youssef, N. N. Jarenwattananon, B. J. Archer, J. Mack, M. L. Iruela-Arispe, and L.-S. Bouchard, "4-D flow control in porous scaffolds: Toward a next generation of bioreactors," *IEEE Trans. Biomed. Eng.*, vol. 64, no. 1, pp. 61–69, Jan. 2017.
- [3] T. Yasukawa *et al.*, "Electrophoretic cell manipulation and electrochemical gene-function analysis based on a yeast two-hybrid system in a microfluidic device," *Analytical Chem.*, vol. 80, no. 10, pp. 3722–3727, 2008.
- [4] D. R. Albrecht, R. L. Sah, and S. N. Bhatia, "Geometric and material determinants of patterning efficiency by dielectrophoresis," *Biophys. J.*, vol. 87, no. 4, pp. 2131–2147, 2004.
- [5] J. K. Valley, A. T. Ohta, H.-Y. Hsu, S. L. Neale, A. Jamshidi, and M. C. Wu, "Optoelectronic tweezers as a tool for parallel single-cell manipulation and stimulation," *IEEE Trans. Biomed. Circuits Syst.*, vol. 3, no. 6, pp. 424–431, Dec. 2009.
- [6] K. Ito, A. Ito, and H. Honda, "Cell patterning using magnetite nanoparticles and magnetic force," *Biotechnol. Bioeng.*, vol. 97, no. 5, pp. 1309–1317, 2007.
- [7] J. El-Ali, P. K. Sorger, and K. F. Jensen, "Cells on chips," *Nature*, vol. 442, no. 7101, pp. 403–411, 2006.
- [8] P. Cheng, P. M. Oliver, M. J. Barrett, and D. Vezenov, "Progress toward the application of molecular force spectroscopy to dna sequencing," *Electrophoresis*, vol. 33, no. 23, pp. 3497–3505, 2012.
- [9] J. J. Messner, H. L. Glenn, and D. R. Meldrum, "Laser-fabricated cell patterning stencil for single cell analysis," *BMC Biotechnol.*, vol. 17, no. 1, pp. 89–97, 2017.
- [10] D. J. Collins, B. Morahan, J. Garcia-Bustos, C. Doerig, M. Plebanski, and A. Neild, "Two-dimensional single-cell patterning with one cell per well driven by surface acoustic waves," *Nature Commun.*, vol. 6, pp. 8686–8696, 2015.
- [11] Y. Yang, Y. Mao, K.-S. Shin, C. O. Chui, and P.-Y. Chiou, "Self-locking optoelectronic tweezers for single-cell and microparticle manipulation across a large area in high conductivity media," *Sci. Rep.*, vol. 6, 2016, Art. no. 22630.
- [12] Z. Huan, H. K. Chu, J. Yang, and D. Sun, "Characterization of a honeycomb-like scaffold with dielectrophoresis-based patterning for tissue engineering," *IEEE Trans. Biomed. Eng.*, vol. 64, no. 4, pp. 755–764, Apr. 2017.
- [13] C. de la Rosa, P. A. Tilley, J. D. Fox, and K. V. Kaler, "Microfluidic device for dielectrophoresis manipulation and electrodisruption of respiratory pathogen bordetella pertussis," *IEEE Trans. Biomed. Eng.*, vol. 55, no. 10, pp. 2426–2432, Oct. 2008.
- [14] P. R. Gascoyne and J. Vykovakal, "Particle separation by dielectrophoresis," *Electrophoresis*, vol. 23, no. 13, pp. 1973–1983, 2002.

- [15] H. A. Pohl, *Dielectrophoresis: The Behavior of Neutral Matter in Nonuniform Electric Fields* (Cambridge Monographs on Physics). Cambridge, U.K.: Cambridge Univ. Press, 1978.
- [16] W. M. Arnold and N. R. Franich, "Cell isolation and growth in electric-field defined micro-wells," *Current Appl. Phys.*, vol. 6, no. 3, pp. 371–374, 2006.
- [17] K. Khoshmanesh *et al.*, "Dielectrophoretic manipulation and separation of microparticles using curved microelectrodes," *Electrophoresis*, vol. 30, no. 21, pp. 3707–3717, 2009.
- [18] S. B. Asokan, L. Jawerth, R. L. Carroll, R. Cheney, S. Washburn, and R. Superfine, "Two-dimensional manipulation and orientation of actin-myosin systems with dielectrophoresis," *Nano Lett.*, vol. 3, no. 4, pp. 431–437, 2003.
- [19] N. Mittal, A. Rosenthal, and J. Voldman, "ndep microwells for single-cell patterning in physiological media," *Lab Chip*, vol. 7, no. 9, pp. 1146–1153, 2007.
- [20] P. R. Gascoyne and J. V. Vykovakal, "Dielectrophoresis-based sample handling in general-purpose programmable diagnostic instruments," *Proc. IEEE*, vol. 92, no. 1, pp. 22–42, Jan. 2004.
- [21] C. Iliescu, L. Yu, F. E. Tay, and B. Chen, "Bidirectional field-flow particle separation method in a dielectrophoretic chip with 3D electrodes," *Sensors Actuators B, Chem.*, vol. 129, no. 1, pp. 491–496, 2008.
- [22] J. Auerswald and H. F. Knapp, "Quantitative assessment of dielectrophoresis as a micro fluidic retention and separation technique for beads and human blood erythrocytes," *Microelectron. Eng.*, vol. 67, pp. 879–886, 2003.
- [23] L. Wang, J. Lu, S. A. Marchenko, E. S. Monuki, L. A. Flanagan, and A. P. Lee, "Dual frequency dielectrophoresis with interdigitated sidewall electrodes for microfluidic flow-through separation of beads and cells," *Electrophoresis*, vol. 30, no. 5, pp. 782–791, 2009.
- [24] Y.-K. Cho, S. Kim, K. Lee, C. Park, J.-G. Lee, and C. Ko, "Bacteria concentration using a membrane type insulator-based dielectrophoresis in a plastic chip," *Electrophoresis*, vol. 30, no. 18, pp. 3153–3159, 2009.
- [25] T. Heida, W. L. Rutten, and E. Marani, "Dielectrophoretic trapping of dissociated fetal cortical rat neurons," *IEEE Trans. Biomed. Eng.*, vol. 48, no. 8, pp. 921–930, Aug. 2001.
- [26] K. Ino, H. Shiku, F. Ozawa, T. Yasukawa, and T. Matsue, "Manipulation of microparticles for construction of array patterns by negative dielectrophoresis using multilayered array and grid electrodes," *Biotechnol. Bioeng.*, vol. 104, no. 4, pp. 709–718, 2009.
- [27] N. Manaresi *et al.*, "A CMOS chip for individual cell manipulation and detection," in *Proc. Solid-State Circuits Int. Conf., Digest Tech. Papers*, 2003, pp. 192–487.
- [28] H. O. Fatoyinbo, D. Kamchis, R. Whattingham, S. L. Ogin, and M. P. Hughes, "A high-throughput 3-D composite dielectrophoretic separator," *IEEE Trans. Biomed. Eng.*, vol. 52, no. 7, pp. 1347–1349, Jul. 2005.
- [29] M. Suzuki, T. Yasukawa, H. Shiku, and T. Matsue, "Negative dielectrophoretic patterning with colloidal particles and encapsulation into a hydrogel," *Langmuir*, vol. 23, no. 7, pp. 4088–4094, 2007.
- [30] M. Suzuki, T. Yasukawa, H. Shiku, and T. Matsue, "Negative dielectrophoretic patterning with different cell types," *Biosensors Bioelectron.*, vol. 24, no. 4, pp. 1043–1047, 2008.
- [31] B. Yafouz, N. A. Kadri, and F. Ibrahim, "The design and simulation of a planar microarray dot electrode for a dielectrophoretic lab-on-chip device," *Int. J. Electrochem. Sci.*, vol. 7, no. 12, pp. 12054–12063, 2012.
- [32] H. Kim *et al.*, "Single-neuronal cell culture and monitoring platform using a fully transparent microfluidic dep device," *Sci. Rep.*, vol. 8, no. 1, 2018, Art. no. 13194.
- [33] N. Couniot, L. A. Francis, and D. Flandre, "A 16×16 CMOS capacitive biosensor array towards detection of single bacterial cell," *IEEE Trans. Biomed. Circuits Syst.*, vol. 10, no. 2, pp. 364–374, Apr. 2016.
- [34] F. J. O'brien, "Biomaterials & scaffolds for tissue engineering," *Mater. Today*, vol. 14, no. 3, pp. 88–95, 2011.
- [35] S.-J. Lee, W. Zhu, L. Heyburn, M. Nowicki, B. Harris, and L. G. Zhang, "Development of novel 3-D printed scaffolds with core-shell nanoparticles for nerve regeneration," *IEEE Trans. Biomed. Eng.*, vol. 64, no. 2, pp. 408–418, Feb. 2017.
- [36] K. Osada, M. Hosokawa, T. Yoshino, and T. Tanaka, "Monitoring of cellular behaviors by microcavity array-based single-cell patterning," *Analyst*, vol. 139, no. 2, pp. 425–430, 2014.
- [37] T. Yue, M. Nakajima, H. Tajima, and T. Fukuda, "Fabrication of microstructures embedding controllable particles inside dielectrophoretic microfluidic devices," *Int. J. Adv. Robot. Syst.*, vol. 10, no. 2, pp. 132–140, 2013.
- [38] K. Huang, H. K. Chu, B. Lu, J. Lai, and L. Cheng, "Automated cell patterning system with a microchip using dielectrophoresis," in *Proc. Int. Conf. Robot. Autom.*, 2019, pp. 634–639.
- [39] K. Huang, H. K. Chu, B. Lu, and L. Cheng, "Characterization of a microchip device for cell patterning via negative dielectrophoresis," in *Proc. IEEE Int. Conf. Robot. Biomimetics*, 2018, pp. 1521–1526.
- [40] Z. Benko, R. T. Elder, G. Li, D. Liang, and R. Y. Zhao, "HIV-1 protease in the fission yeast *schizosaccharomyces pombe*," *Plos One*, vol. 11, no. 3, 2016, Art. no. e0151286.
- [41] Y. Huang, R. Holzel, R. Pethig, and X.-B. Wang, "Differences in the ac electrodynamics of viable and non-viable yeast cells determined through combined dielectrophoresis and electrorotation studies," *Phys. Med. Biol.*, vol. 37, no. 7, 1992, Art. no. 1499.
- [42] N. Flores-Rodriguez and G. H. Markx, "Improved levitation and trapping of particles by negative dielectrophoresis by the addition of amphoteric molecules," *J. Phys. D, Appl. Phys.*, vol. 37, no. 3, pp. 353–361, 2004.
- [43] S. D'souza, J. Melo, A. Deshpande, and G. Nadkarni, "Immobilization of yeast cells by adhesion to glass surface using polyethylenimine," *Biotechnol. Lett.*, vol. 8, no. 9, pp. 643–648, 1986.
- [44] K. V. Goossens and R. G. Willaert, "The N-terminal domain of the Flo11 protein from *saccharomyces cerevisiae* is an adhesin without mannose-binding activity," *FEMS Yeast Res.*, vol. 12, no. 1, pp. 78–87, 2012.
- [45] K. J. Verstrepen and F. M. Klis, "Flocculation, adhesion and biofilm formation in yeasts," *Mol. Microbiol.*, vol. 60, no. 1, pp. 5–15, 2006.
- [46] J. C. Bayly, L. M. Douglas, I. S. Pretorius, F. F. Bauer, and A. M. Dranginis, "Characteristics of Flo11-dependent flocculation in *saccharomyces cerevisiae*," *FEMS Yeast Res.*, vol. 5, no. 12, pp. 1151–1156, 2005.
- [47] J. T. Decker *et al.*, "Engineered antifouling microtopographies: An energetic model that predicts cell attachment," *Langmuir*, vol. 29, no. 42, pp. 13023–13030, 2013.
- [48] A. Singh *et al.*, "Bottom-up engineering of the surface roughness of nanostructured cubic zirconia to control cell adhesion," *Nanotechnology*, vol. 23, no. 47, 2012, Art. no. 475101.
- [49] K. Anselme and M. Bigerelle, "Effect of a gold–palladium coating on the long-term adhesion of human osteoblasts on biocompatible metallic materials," *Surf. Coatings Technol.*, vol. 200, no. 22/23, pp. 6325–6330, 2006.
- [50] D. D. Deligianni, N. D. Katsala, P. G. Koutsoukos, and Y. F. Missirlis, "Effect of surface roughness of hydroxyapatite on human bone marrow cell adhesion, proliferation, differentiation and detachment strength," *Biomaterials*, vol. 22, no. 1, pp. 87–96, 2000.
- [51] S. Giljean, M. Bigerelle, and K. Anselme, "Roughness statistical influence on cell adhesion using profilometry and multiscale analysis," *Scanning*, vol. 36, no. 1, pp. 2–10, 2014.
- [52] H.-H. Huang, C.-T. Ho, T.-H. Lee, T.-L. Lee, K.-K. Liao, and F.-L. Chen, "Effect of surface roughness of ground titanium on initial cell adhesion," *Biomolecular Eng.*, vol. 21, no. 3/5, pp. 93–97, 2004.
- [53] Y. Shen, M. R. Ahmad, M. Nakajima, S. Kojima, M. Homma, and T. Fukuda, "Evaluation of the single yeast cell's adhesion to ito substrates with various surface energies via esem nanorobotic manipulation system," *IEEE Trans. Nanobiosci.*, vol. 10, no. 4, pp. 217–224, Dec. 2011.
- [54] S. H. Tan, N.-T. Nguyen, Y. C. Chua, and T. G. Kang, "Oxygen plasma treatment for reducing hydrophobicity of a sealed polydimethylsiloxane microchannel," *Biomicrofluidics*, vol. 4, no. 3, 2010, Art. no. 032204.
- [55] F. Dong, M. Zhang, W. Huang, L. Zhou, M.-S. Wong, and Y. Wang, "Superhydrophobic/hydrophobic nanofibrous network with tunable cell adhesion: Fabrication, characterization and cellular activities," *Colloids Surf. A, Physicochem. Eng. Aspects*, vol. 482, pp. 718–723, 2015.
- [56] M. Mercier-Bonin, K. Ouazzani, P. Schmitz, and S. Lorthois, "Study of bioadhesion on a flat plate with a yeast/glass model system," *J. Colloid Interface Sci.*, vol. 271, no. 2, pp. 342–350, 2004.
- [57] D. P. Dowling, I. S. Miller, M. Ardhaoui, and W. M. Gallagher, "Effect of surface wettability and topography on the adhesion of osteosarcoma cells on plasma-modified polystyrene," *J. Biomater. Appl.*, vol. 26, no. 3, pp. 327–347, 2011.



**Kaicheng Huang** received the B.Eng. degree from the Department of Automation, Shenzhen University, Shenzhen, China, in 2014, and the M.Sc. degree in mechanical and automation engineering from The Chinese University of Hong Kong, Hong Kong, China, in 2015. He is currently working toward the Ph.D. degree with the Hong Kong Polytechnic University, Hong Kong. His research interests include automated cell patterning with dielectrophoresis and micro manipulation.



**Bo Lu** received the B.Eng. degree from the Dalian University of Technology, Dalian Shi, China, in 2013, and the M.S. degree (first honor) from The Hong Kong Polytechnic University, Hong Kong, in 2015. He is currently working toward the Ph.D. degree with the Department of Mechanical Engineering, The Hong Kong Polytechnic University, Hong Kong. His current research interests include surgical robots, automation and control, trajectory plan, computer vision, surgical tool detection.



**Henry Kar Hang Chu** (M'12) received the B.S. degree in mechanical engineering from the University of Waterloo, Waterloo, ON, Canada, and the M.S. and Ph.D. degrees in mechanical and industrial engineering from the University of Toronto, Toronto, ON, Canada. He was a Postdoctoral Fellow with the University of Toronto and the City University of Hong Kong, Hong Kong. He is currently an Assistant Professor with The Hong Kong Polytechnic University, Hong Kong. His research interests include robotic manipulation, vision-based control and automation, microsystem design, and tissue engineering.



**Jiewen Lai** received the B.Eng. degree from the Department of Metallurgical Engineering, Wuhan University of Science and Technology, Wuhan, China, in 2016, and the M.Sc. degree from the Department of Mechanical and Automation Engineering, The Chinese University of Hong Kong, Hong Kong, in 2017. He is currently working toward the Ph.D. degree with The Hong Kong Polytechnic University, Hong Kong. His research interests include continuum robot, soft robot, robotic control, and computer vision.